Carbohydrate Polymers 90 (2012) 419–430

Contents lists available at SciVerse ScienceDirect

Carbohydrate Polymers

journal homepage: www.elsevier.com/locate/carbpol

# Photocrosslinking, micropatterning and cell adhesion studies of sodium hyaluronate with a trisdiazonium salt

Miguel Lomba[a], Luis Oriol[a,*], Carlos Sánchez[b,**], Valeria Grazú[c], Berta Sáez Gutiérrez[c,d], José Luis Serrano[c], Jesús Martínez De la Fuente[c]

[a] Instituto de Ciencia de Materiales de Aragón (ICMA), CSIC-Universidad de Zaragoza, Departamento de Química Orgánica, Facultad de Ciencias, C./Pedro Cerbuna 12, 50009 Zaragoza, Spain
[b] Instituto de Ciencia de Materiales de Aragón (ICMA), CSIC-Universidad de Zaragoza, Departamento de Física de la Materia Condensada, Facultad de Ciencias, C./Pedro Cerbuna 12, 50009 Zaragoza, Spain
[c] Instituto Universitario de Nanociencia de Aragón, Campus Río Ebro (Edificio I+D), 50018 Zaragoza, Spain
[d] Instituto Aragonés de Ciencias de la Salud, Avenida Gómez Laguna, 50009 Zaragoza, Spain

ARTICLE INFO

*Article history:*
Received 27 January 2012
Received in revised form 7 May 2012
Accepted 19 May 2012
Available online 28 May 2012

In memory of Professor Carmen Peinado.

*Keywords:*
Sodium hyaluronate
Microstructuring
Photopolymerization
Cell adhesion
Diazonium salt

ABSTRACT

Chemically unmodified sodium hyaluronate has been crosslinked by photoinduced decomposition of a trifunctional diazonium salt to generate new biomaterials. In addition, the photocrosslinking process does not require a photoinitiator. Thin films of formulations of sodium hyaluronate and the photocrosslinker at different percentages have been processed. Cytotoxicity has been explored and toxicity was not observed with the selected cell lines. 2D patterns of controlled geometry have been generated by direct laser writing to perform cell adhesion studies. Different adhesion behavior of the cell lines, as assessed by vinculin immunostaining and scanning electron microscopy, has been observed in the polymeric films depending on the degree of photocrosslinking.



## 1. Introduction

Natural polymers are widely investigated as biomaterials due to their intrinsic attractive properties for biomedical applications. These materials can show biological activity in stimulating cell response events such as signaling, differentiation, adhesion, proliferation and migration (Dutta & Dutta, 2010; Friedl, Zänker, & Bröcker, 1998). An example of a natural polymer is hyaluronic acid (HA) and its salt derivatives. HA is a high molecular weight glycosaminoglycan that is ubiquitously found in the connective tissues of mammals, such as vitreous humor, synovial fluids and umbilical cord. HA is involved in biological processes such as angiogenesis (Perng, Wang, Tsi, & Ma, 2011; Raines et al., 2011), organ morphogenesis (Masters, Shah, Leinwand, & Anseth, 2005) and wound healing (Chen & Abatangelo, 1999). In addition this natural polymer is intrinsically biodegradable, serving this as an important advantage in biomedical applications (Burdick & Prestwich, 2011; Gomes & Reis, 2004). These inherent biological characteristics make HA an attractive platform for the preparation of biomaterials, and significant effort has been focused on modifying its chemical structure in an effort to tune its properties (Badylak, Freytes, & Gilbert, 2009; Malafaya, Silva, & Reis, 2007; Rinaudo, 2008). In particular, the chemical modification of HA and its subsequent crosslinking to obtain biomaterials of interest as scaffolds for tissue engineering (Camci-Unal et al., 2010; Lei, Gojgini, Lam, & Segura, 2011; Masters et al., 2005; Nuernberger et al., 2011) or systems for drug delivery (Inukai, Jin, Yomota, & Yonese, 2000; Patterson et al., 2010) has been widely investigated.

The functional groups found in HA have allowed the development of different crosslinking strategies. In this way, HA has been crosslinked by using carbodiimides (Tomihata & Ikada, 1997) or dihydrazides (Vercruysse, Marecak, Marecek, & Prestwich, 1997). HA has also been functionalized with acrylic or methacrylic groups to be subsequently crosslinked by radical polymerization (Kutty, Cho, Lee, & Vyavahare, 2007; Masters et al., 2005) or by Michael-type addition reaction with multifunctional thiols (Kim et al., 2009; Lei et al., 2011). Studies carried out on this kind of crosslinked

* Corresponding author. Tel.: +34 976762276; fax: +34 976239302.
** Corresponding author. Tel.: +34 976763353; fax: +34 976761229.
*E-mail addresses:* mlomba@unizar.es (M. Lomba), loriol@unizar.es (L. Oriol), carloss@unizar.es (C. Sánchez), vgrazu@unizar.es (V. Grazú), bsaez@unizar.es (B.S. Gutiérrez), joseluis@unizar.es (J.L. Serrano), jmfuente@unizar.es (J.M. De la Fuente).

0144-8617/$ – see front matter © 2012 Elsevier Ltd. All rights reserved.
http://dx.doi.org/10.1016/j.carbpol.2012.05.061

system have shown for example that a change in the degree of methacrylation, and therefore in the crosslinking degree, has a large impact on the mechanical properties of the material while retaining the biocompatibility (Bencherif et al., 2008).

Among the different HA crosslinking strategies, those induced by light are of particular interest for the generation of biomaterials (Hoare & Kohane, 2008; Oh, Drumright, Siegwart, & Matyjaszewski, 2008; Van Tomme, Storm, & Hennink, 2008). Photoinduced polymerization allows the in situ preparation of biomaterials. Besides, by using photolithographic techniques it is possible to create structures with specific geometries (Bratton, Yang, Dai, & Ober, 2006) that could locally control cell adhesion and guide cell proliferation (Khetan & Burdick, 2011; Nuernberger et al., 2011; Seidlits, Schmidt, & Shear, 2009).

Photocrosslinking of HA has been mainly performed by light-initiated radical photopolymerization of acrylate-modified HA (Kutty et al., 2007; Masters et al., 2005). This process leads to acrylic non biodegradable chains that may become difficult to eliminate from the body (Baroli, 2006). Alternatives to this acrylate-based photochemistry, that could circumvent this drawback, are thiol-ene (Hoyle & Bowman, 2010) or thiol-yne (Lowe, Hoyle, & Bowman, 2010) photochemistry, which have been already used in biopolymers (Censi, Fieten, di Martino, Hennink, & Vermonden, 2010; Ji et al., 2006; Lei et al., 2011; Lomba et al., 2011). Step growth polymerization in these systems leads to homogeneously crosslinked networks and this avoids the formation of acrylic non biodegradable chains (Rhydolm, Bowman, & Anseth, 2005; Rhydolm, Reddy, Anseth, & Bowman, 2007; Senyurt, Wei, Hoyle, Piland, & Gould, 2007). Nevertheless the application of this chemistry to HA also requires the prior chemical modification of hyaluronic polymeric chains with reactive groups.

Alternative photocrosslinking reactions that can be directly performed with chemically unmodified natural polymers are of interest in biomaterials. The crosslinking reaction based on the photodecomposition of aromatic diazonium salts could be an interesting choice. The photocrosslinking reaction involves the photoinduced decomposition of aromatic diazonium groups to give an aromatic carbocation (Cao, Zhao, & Cao, 1998) that can react with a nucleophilic group such as sulfonate (Cao, Ye, Cao, & Zhao, 1997; Sun et al., 1998; Zhang & Cao, 2000), carboxylate (Cao et al., 2001a; Zhao, Zhang, Yang, Sun, & Sun, 2006), or hydroxyl groups (Chen & Cao, 1999), commonly found in natural polymers. So far, this reaction has been widely studied for the fabrication of negative presensitized plates (Liu, Lee, & Tsai, 1998; Zhang & Cao, 2000) and electrooptical devices (Cao, Yang, Cao, et al., 2001; Cao, Yang, Yang, Huang, & Cao, 2001; Zhang, Peng, Yao, Ly, & Xuan, 2007; Zhao et al., 2006), by using polymeric diazonium salts as photocrosslinker to react with synthetic polymers bearing nucleophilic groups. These polymeric diazonium salts have also been used in the crosslinking of polymers for biological applications such as the generation of microspheres for the encapsulation of enzymes (Srivastava, Brown, Zhu, & McShane, 2005) or the crosslinking of DNA as a suitable technique for the generation of DNA arrays (Yu et al., 2006) or biosensors (Li, Ouyang, Chen, Zhao, & Cao, 2002). This photoreaction can be applied to the photocrosslinking of natural polymers without the need for prior chemical modification of the polymer. In order to generate fully degradable materials, the use of a non-polymeric diazonium salt would be appropriate since degradation of the crosslinked material would lead to low molecular weight residues.

In the present work the photocrosslinking of chemically unmodified sodium hyaluronate was carried out with a trifunctional diazonium salt derived from triphenylamine to give a polymeric network (Scheme 1). The photocrosslinkable polymeric formulations can be prepared from aqueous solutions due to the ionic or polar nature of the compounds. Furthermore, the photocrosslinking in these systems occurs without the need for a photoinitiator which could be toxic itself or generate side-products that could be toxic for cells (Baroli, 2006; Fridovich, 1998).

The reactivity of the crosslinker with hydroxyl and carboxylate groups, both of which are found in sodium hyaluronate, was checked by using sodium polyacrylate (PAANa) and poly(vinyl alcohol) (PVA) as model polymers. Afterwards, the photocrosslinking of sodium hyaluronate, that contains these functional groups, was studied by UV–vis and FTIR spectroscopies. The biocompatibility of the polymeric materials obtained by photocrosslinking of hyaluronic chains with the trifunctional diazonium salt crosslinker was studied by MTT cell proliferation assays. 2D patterned structures were generated by direct laser writing (DLW) in order to study the adhesion of cells to the micropatterned polymeric material.

## 2. Experimental

### 2.1. Materials

Poly(acrylic acid, sodium salt) (PAANa) from Polyscience Europe GmbH (Mn ≈ 225,000 Da, 20% solution in water) and poly(vinyl alcohol) (PVA) from Aldrich (Mn ≈ 65,000 Da) were used as model polymers to check the photoreaction. Sodium hyaluronate (Hyal, Mn ≈ 1,000,000 Da) from Acros Organics was used as the natural polymer. All polymers were used as received. As crosslinker, the diazonium salt derived from tri(4-aminophenyl)amine (ORGANICA) was used and prepared by diazotization with $NaNO_2$ as described previously (Lomba, Oriol, & Sánchez, 2009).

Cell studies were performed with HeLa (human cervical carcinoma) tumoral cells and COS-7 fibroblasts (African Green Monkey SV40-transfected kidney fibroblasts). HeLa tumoral cells were donated by Hospital Puerta de Hierro (Madrid, Spain) and COS-7 fibroblasts were obtained from ATCC.

Dulbecco's Modified Eagle's Medium DMEM (Lonza) was used as culture medium. DMEM was supplemented with 10% fetal bovine serum (FBS), 1% glutamine and 1% penicillin/streptomycin. The cells were incubated at 37 °C with a 5% $CO_2$ atmosphere for the desired time onto round glass coverslips (Marienfeld GmbH, 12 mm diameter).

For viability assays, (3-(4,5-dimethylthiazol-2-yl)-2,5-diphenyltetrazolium) bromide (MTT, Sigma) was dissolved in phosphate buffer solution (PBS, 5 mg/mL) and diluted 1:20 with complete culture medium (50 μL of MTT in PBS and 950 μL of complete culture medium).

For cell cytoskeleton fluorescent staining, 4% formaldehyde (Sigma Aldrich)/PBS with 1% sucrose was used as a fixative buffer. Permeabilizing buffer was prepared by dissolving 10.3 g sucrose (Sigma), 0.292 g NaCl (Panreac), 0.06 g $MgCl_2$ hexahydrate (Panreac), 0.476 g Hepes (Sigma) in 100 mL PBS; subsequently, the pH was adjusted to pH 7.2 and 0.5 mL of Triton X (Panreac) were added. Bovine serum albumin (BSA) buffer was prepared by dissolving 1 g of BSA (Sigma) in 100 mL of PBS and washing buffer was prepared by dissolving 0.5 mL of Tween 20 (Panreac) in 100 mL of PBS. Monoclonal anti-human raised in mouse (IgG1) antibody was purchased from Sigma and used as the primary antibody for vinculin fluorescent staining. Biotinylated monoclonal anti-mouse (IgG) from Vector Laboratories was used as secondary antibody. Texas Red-conjugated streptavidin from Vector Laboratories was used as a fluorescent marker. Alexa Fluor® 488 Phalloidin conjugate was purchased from Invitrogen and used for actin fluorescent staining. 2-(4-Amidinophenyl)-6-indolecarbamidine dihydrochloride (DAPI) was used as a nuclear fluorescent staining agent and was dissolved in PBS (5 mg/mL) and diluted 1:10,000 prior to incubation. Prolong® Gold Antifade Reagent from Invitrogen was used as mounting medium.

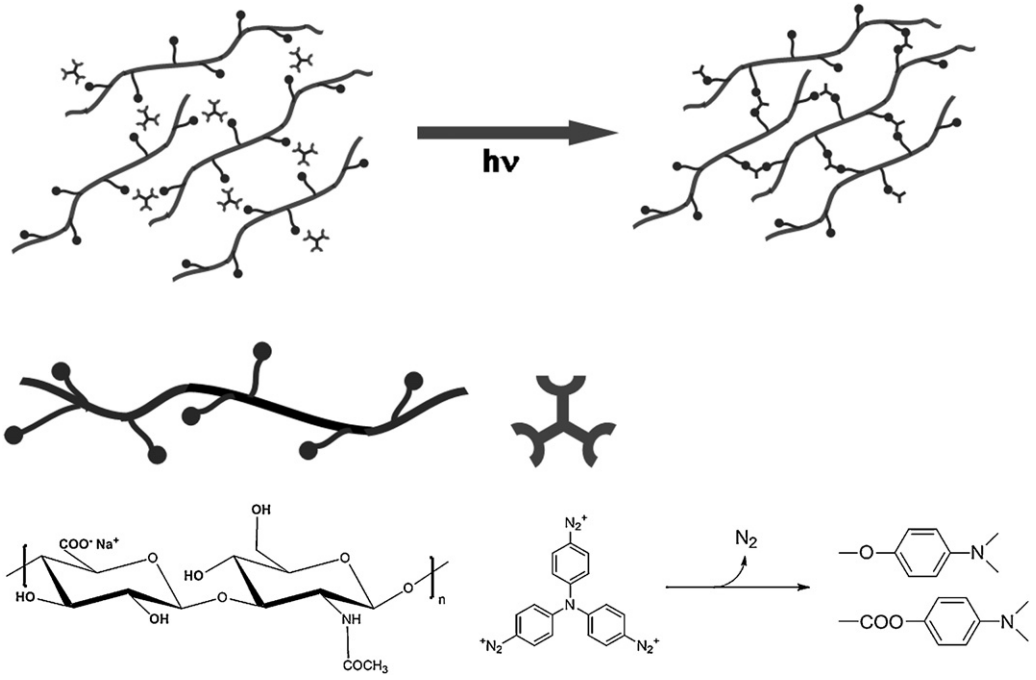


**Scheme 1.** Photoinduced crosslinking of sodium hyaluronate under irradiation with UV light using a trisdiazonium salt.

For morphological characterization by SEM microscopy, 2.5% glutaraldehyde (Sigma–Aldrich)/PBS was used as fixative buffer.

### 2.2. Films preparation

Photocrosslinkable thin films were prepared from formulations of the polymers and the diazonium salt-based photocrosslinker to yield a controlled composition (expressed as weight percentage of the crosslinker). The diazonium salt was generated in situ in an aqueous solution as reported previously (Lomba et al., 2009) and combined with a solution of the polymer in water.

30 wt% of crosslinker was used for the photocrosslinkable formulations of the model polymers sodium polyacrylate (PAA 30) and poly(vinyl alcohol) (PVA 30). Sodium hyaluronate was combined with 5 wt% (H5) and 20 wt% (H20) of the trisdiazonium salt crosslinker.

These formulations were spin-coated (two step programs: 1000 rpm for 5 s and 3000 rpm for 100 s except for sodium hyaluronate for which the second step was extended to 300 s to ensure evaporation) onto clean glass substrates (previously exposed to ozone treatment for several minutes) for UV characterization and calcium fluoride substrates for IR characterization. For cell studies, thin films were prepared on round glass coverslips of 12 mm diameter, also exposed to ozone treatment for several minutes.

### 2.3. Photocrosslinking process

Flood-exposed films were used for UV–vis and FTIR spectroscopies, and for cell viability assays. 2D-patterned structures, obtained by direct laser writing (DLW) and subsequent wet etching of the unexposed areas, were used in cell adhesion studies. Two different light sources were used depending on the experiment to be performed. A 300 W Mercury lamp (from Oriel, Model #6286; Lamp Housing also from Oriel, Model #66902) in conjunction with a UV reflecting filter (Oriel, Model #66218) was used as a light source for flood-exposed films. These samples were irradiated for 2 min with a UV light intensity of 160 mW/cm$^2$ (350–450 nm). A focused laser beam of 405 nm was used for DLW experiments. The laser beam (diameter: 1.7 mm, Intensity: 1.75 mW) was focused by a 40× UV microscope objective onto the sample. By moving the film in the *XY* plane, lines of the photocrosslinkable film can selectively be photocrosslinked. The unreacted areas were removed by dipping and gently moving the film in 0.06 M aqueous NaOH for 10 s and subsequent fluxing with water. Finally, the films were dried under an air flow.

### 2.4. Cell viability assays

Cell studies were performed by culturing HeLa tumoral cells and COS-7 fibroblasts onto films of crosslinked polymeric material deposited on round glass coverslips (12 mm diameter). HeLa tumoral cells or COS-7 fibroblasts were seeded at the corresponding density of cells per disk in 1 mL of complete culture medium. Cell viability and proliferation were analyzed by the MTT colorimetric assay (Mosmann, 1983). Flood-exposed substrates of the different polymeric materials were first sterilized with 70% ethanol for 15 min and subsequently washed with sterilized PBS for another 15 min. Substrates were cultured in wells of a 24-well titer plate with 50,000 cells (HeLa tumoral cells and COS-7 fibroblasts) per 1 mL of complete culture medium, and grown for 24, 48 and 72 h (five different samples for each culture period). After cells had been cultured for the selected time, substrates were transferred to another 24-well titer plate and they were incubated with 1 mL of diluted MTT dye solution. After 4 h of incubation at 37 °C in 5% $CO_2$, the medium was removed and the resulting formazan crystals were dissolved in 1 mL of dimethyl sulfoxide (DMSO). Aliquots of 200 μL of solution were taken for absorbance measurements and these were carried out on a microplate reader (Biotek ELX800) at 570 nm. The spectrophotometer was calibrated to zero absorbance using DMSO. The same process was performed with substrates of polymeric material cultured without cells (as negative control) to correct from measured absorbance any possible contribution not related with formazan-crystals generated in MTT metabolism.

The cell viability (%), relative to control wells containing cells cultured onto bare glass substrate (viability control), was calculated by the formula $[A]_{test}/[A]_{control} \times 100$, where $[A]_{control}$ is the absorption of formazan generated by the cells growth on the glass substrate control and $[A]_{test}$ is the absorption of formazan generated by the cells growth on the sample after subtracting the absorbance of the negative control (substrates without cells). This experiment was repeated at least five times for each sample in order to obtain the average and the standard deviation.

### 2.5. Cell adhesion studies

For adhesion studies, substrates of polymeric material patterned on glass were sterilized with 70% ethanol for 15 min and subsequently washed with PBS solution for another 15 min as performed for cell proliferation assays. These substrates of patterned polymeric material were cultured in 24-well titer plates with 1 mL of culture medium with a density of 10,000 (HeLa tumoral cells and COS-7 fibroblasts) cells per well.

After the desired culture time, cells adhered onto patterned polymeric material substrates were fixed with 4% formaldehyde fixative buffer at 37 °C for 15 min. The samples were then washed with PBS and incubated with permeabilizing buffer at 4 °C for 5 min prior to being incubated for 5 min in blocking buffer at 37 °C. For vinculin fluorescent staining, the permeabilizing step was followed by the addition of anti-vinculin primary antibody for 1 h at 37 °C. The samples were then washed with washing buffer and the secondary antibody was added for 1 h at 37 °C followed by another washing step. Texas Red marker was added at 4 °C for 30 min followed by a final wash. For actin fluorescent staining, the permeabilizing step was followed by incubation with Alexa Fluor® 488-conjugated phalloidin for 1 h at 37 °C. All antibodies and markers were diluted 1:50 in blocking buffer. Finally, coverslips were incubated with DAPI for 5 min at room temperature (RT), washed with distilled water and mounted with Prolong® Gold Antifade Reagent before being viewed using the confocal scanning microscope.

### 2.6. Sequential microscopy of HeLa cells cultured on H5 patterns

Sequential microscopy experiments were carried out for *in* vivo monitoring of HeLa tumoral cells when cultured onto H5 polymeric patterns. For these experiments, glass substrates with H5 polymeric pattern were sterilized with 70% ethanol for 15 min and subsequently washed with PBS solution for another 15 min as was done for cell proliferation assays. Subsequently, substrates were fixed to a Petri plate of cell culture (μ-Dish for Live Cell analysis; Ibidi) with fibronectin, which was let drying for several hours in a sterile environment.

HeLa tumoral cells were cultured for 24 h in a chamber at 37 °C and 5% $CO_2$ with a density of 20,000 cells in 2 mL of culture medium. During this period, differential interference contrast (DIC) images were taken every 15 min in different points of the sample.

### 2.7. Morphological characterization by SEM microscopy

For morphological characterization of cells by SEM microscopy, flood-exposed films of polymeric material H5 or glass substrates were sterilized with 70% ethanol for 15 min and subsequently washed with PBS solution for another 15 min as was done for cell proliferation assays. These substrates were cultured into 24-well titer plates with 1 mL of culture medium with a density of 20,000 (HeLa tumoral cells and COS-7 fibroblasts) cells per well.

After the desired culture time, cells adhered onto the flood-exposed polymeric film or the glass substrate were fixed with 2.5% glutaraldehyde fixative buffer at 4 °C for 1 h. The samples were then washed with PBS at 4 °C for 20 min three times and, subsequently, washed with distilled water at 4 °C for 20 min other three times. The dehydration process was carried out by successive incubation at 4 °C for 10 min in 25%, 50%, 70%, 90% and 100% ethanol (incubation with 100% ethanol was repeated twice). Finally, samples were coated with approximately 15 nm of gold to obtain a conducting sample.

### 2.8. Flow cytometry analysis

Flow cytometry analyses were carried out by culturing HeLa tumoral cells or COS-7 fibroblasts onto films of crosslinked polymeric material H5 deposited on round glass coverslips (12 mm diameter) or cultured onto the bare glass coverslips (as control). HeLa tumoral cells or COS-7 fibroblasts were seeded in a 24-well titer plate at a density of 100,000 cells per disk in 1 mL of complete culture medium. After 24 h of incubation, substrates were transferred to another 24-well titer plate and cells were detached by incubation with 100 μL of trypsin (2 min at 37 °C and 5% $CO_2$), which was subsequently neutralized with 1 mL of complete medium (this experiment was repeated on 20 samples). Cells from all samples were combined and centrifuged at $300 \times g$ for 7 min. Supernatant culture medium was decanted off and cells were suspended again in 200 μL of PBS to be fixed with 1 mL of cold EtOH (−20 °C) overnight at 4 °C. Cells were centrifuged at $300 \times g$ for 7 min, washed with 500 μL of PBS and centrifuged again at $300 \times g$ for 7 min. Finally cells were stained with 1 mL of staining solution (50 μg/mL of propidium iodide and 100 μg/mL of RNAsa in PBS) during 30 min in darkness at room temperature.

### 2.9. Equipment and characterization techniques

UV–vis spectra were measured using a Varian Cary 500 UV-vis-IR spectrophotometer. FTIR spectra were measured on a Bruker Vertex 70 IR spectrophotometer. Topographic characterization of the 2D patterned structures obtained by the DLW process was performed using a Dual Sensofar PLU 2300 microscope working in confocal mode. For cell proliferation assays, absorbance at 570 nm for MTT was measured on a Biotek ELX800 microplate reader spectrophotometer. The stained sections were visualized with an Olympus FV10i confocal scanning microscope. Images were collected using the microscope in sequential mode with a 60× oil immersion lens (lens specification, UPLSAPO 60×, NA 1.35), a line average of 8 and a format of 1024 pixel × 1024 pixel. The confocal pinhole was 1 Airy unit. For the overall view of the specimen used to locate the observation target (map image), a 10× microscope objective was used (lens specification UPLSAPO 10×, NA 0.4) and 7 × 7 fields were combined into a composite image. For sequential microscopy experiments, cells were cultured into Petri plates of cell culture (μ-Dish for Live Cell analysis; Lomba et al., 2009). Images were collected for 24 h using a Leica AF6000 LX microscope with a chamber that provides a environment at 37 °C and 5% $CO_2$ for cell culture. Images were collected by a CCD camera (Model Orca 9100-02; Hamamatsu) using a 40× HCX PL S-APO objective of differential interference contrast (DIC). Images were collected at intervals of 15 min and saved and processed as set of images using a LAS AF (Leica Microsystems) software. SEM images were collected using a Inspect F50 scanning electron microscopy working at high vacuum ($<6e^{-4}$ Pa) with an accelerating voltage from 200 V to 30 kV. Flow cytometry analyses were carried out using a BD FACSArray cytometer and data were analyzed with Modfit 3.0 software from Verity Software.

## 3. Results and discussion

### 3.1. Photocrosslinking of model polymers

The photoinduced reaction of polymeric diazonium salts has been described for polymers containing sulfonate (Cao et al., 1997; Sun et al., 1998; Zhang & Cao, 2000), carboxylate (Cao et al., 2001a; Zhao et al., 2006) or hydroxyl (Chen & Cao, 1999) groups to yield crosslinked materials. However, the use of a non-polymeric diazonium salt as a photocrosslinker has been much less explored. We recently described the photocrosslinking of poly(styrene sulfonate) (PSS) using a trisdiazonium salt derived from tri(4-aminophenyl)amine, as well as the photopatterning of polymeric films using the photoreaction of the diazonium and the sulfonate groups (Lomba et al., 2009). In an attempt to extend this reaction to polymers containing hydroxyl and carboxylic groups (found in HA), an initial study was carried out using PAANa and PVA as model systems.

The photoreactivity of the trisdiazonium salt with the model polymers PAANa and PVA was checked using formulations with 30 wt% of photocrosslinker (the formulations were coded as PAA 30 and PVA 30). This percentage was selected on the basis of previous work carried out with PSS (Lomba et al., 2009).

The photocrosslinking of films processed from formulations of the model polymers and the diazonium salt (30 wt%) was carried out by flood exposure with UV light, and the resulting materials were characterized by UV–vis and FTIR spectroscopy. Films processed from the photoreactive formulations exhibit an absorption band at 431 nm for the case of PAA 30 (Fig. 1a) and at 435 nm for PVA 30 (Fig. 1b) before irradiation due to the $\pi$–$\pi^*$ transition of the diazonium group. A red shift and a broadening of the absorption band is observed with respect the band of the diazonium salt in solution (Lomba et al., 2009). This could be ascribed to the interaction of the carboxyl and hydroxyl groups of the corresponding polymers with the diazonium salt and to interactions between neighbor crosslinker molecules. This broadening is more pronounced for the PAA than for the PVA photopolymer that could be due to the ionizable character of the carboxyl groups of the first polymer leading to ionic interactions with the diazonium salt. After irradiation this band disappears, as shown in Fig. 1 for PAA 30 (a) and PVA 30 (c), and this change is due to the decomposition of diazonium group (Lomba et al., 2009; Sun et al., 1998; Zhao et al., 2006).

In order to check that the decomposition of the diazonium salt finally results in effective crosslinking of the polymers, FTIR spectroscopic studies were performed before and after irradiation with UV light (Fig. 1b and d). The diazonium group shows an absorption band at around 2260 $cm^{-1}$ and this is assigned to the stretching vibration of the N≡N bond. The band at around 1575 $cm^{-1}$ is assigned to the phenyl groups conjugated to the diazonium groups (Lomba et al., 2009; Zhao et al., 2006). Both signals are affected by UV light irradiation. The first signal disappears, which indicates diazonium decomposition, and the second is shifted to higher wavenumbers due to the loss of conjugation with the diazonium group. The crosslinker shows another two bands at around 1330 and 1290 $cm^{-1}$ that are attributed to the stretching vibration of C—N bonds between the central tertiary amine and the phenyl groups. These groups are also modified upon irradiation with UV light (zoomed region in Fig. S1, supplementary data). Regarding the model polymers, PAANa shows a broad signal at around 1660 $cm^{-1}$ (Fig. 1b) that is assigned to the C=O stretching vibration of the carboxylate groups. After UV irradiation of the photocrosslinkable film PAA 30, a broadening of the band in that region and a shift to higher wavenumber due to the formation of the ester groups (Cao, Yang, Cao, et al., 2001) is observed (see Scheme 1 for chemical reaction). The ester bands are overlapped with the bands due to unreacted carboxylate groups (excess) giving rise to this broadening and shift. On the other hand, PVA (Fig. 1d) shows an absorption band at 1257 that is assigned to the stretching vibration of C—O bonds. After irradiation, a broad band centered around 1250 $cm^{-1}$ and a new band at 1321 $cm^{-1}$ are detected in that region, which are due to the photodecomposition of photocrosslinker and concomitant formation of ether bond as well as unreacted hydroxyl groups (excess). Furthermore, the irradiated films derived from the two model polymers become insoluble in 0.06 M aqueous NaOH solution, a solvent in which the unexposed photocrosslinkable materials easily dissolve. This change in solubility in both photocrosslinkable materials is a macroscopic indication of the effective photocrosslinking process and confirms the reaction of the diazonium salt with the polymeric chains of PAANa and PVA upon UV irradiation.

### 3.2. Photocrosslinking of sodium hyaluronate

After confirming the reactivity of the diazonium salt with hydroxyl and carboxylate groups of the model polymers, the photocrosslinking of sodium hyaluronate with the trisdiazonium salt was investigated. The process was carried out by flood exposure with UV light of photocrosslinkable thin films prepared from sodium hyaluronate and crosslinker formulations.

A non-homogeneous solution of sodium hyaluronate (with a molecular weight of around 1,000,000 Da) was obtained on adjusting the crosslinker percentage to 30 wt%. Therefore, lower crosslinker percentages were studied and photocrosslinkable sodium hyaluronate formulations with 5 wt% (coded as H5) and 20 wt% (coded as H20) of crosslinker were prepared. These formulations led to viscous but homogeneous solutions that allowed the preparation of photocrosslinkable thin films. The photodecomposition of the diazonium salt in formulations H5 and H20 was monitored by UV–vis and similar results were obtained as for the model systems (see Supplementary data, Fig. S2). The band at 412 nm completely disappeared, indicating decomposition of the diazonium group upon irradiation. FTIR spectra (Fig. 2) after irradiation also reveal the appearance of a new signal at 1740 $cm^{-1}$ due to the formation of ester groups. The region 1350–1200 $cm^{-1}$ is also modified by irradiation (a new band at 1323 $cm^{-1}$ and a broad band at around 1250 $cm^{-1}$) due to the photodecomposition of the crosslinker and reaction with hyaluronic polymer (reaction with carboxylate and hydroxyl groups). Films of both formulations, H5 and H20, became insoluble in NaOH [aq] solution after UV light exposure, a change that provides evidence of an effective crosslinking process.

The photoinduced decomposition of diazonium salts can also be extended to the photocrosslinking of other natural polymers containing nucleophilic groups without the need for chemical modification of the natural polymer. For instance, sodium heparin, which contains sulfate groups, was also crosslinked by irradiation of photocrosslinkable films with 30 wt% of crosslinker. The process was also characterized by UV–vis absorption and FTIR spectroscopy (Fig. S3 in supplementary data) which demonstrate the photodecomposition of diazonium group and the formation of the sulfate ester bond.

### 3.3. Biocompatibility of crosslinked sodium hyaluronate

Biocompatibility of crosslinked sodium hyaluronate (having 5% and 20 wt% of crosslinker respectively) was assessed by performing MTT cell proliferation assays (Mosmann, 1983) for different incubation times (24, 48 and 72 h) in UV-light flood-exposed films with two different cell lines: HeLa and COS-7 fibroblasts as tumoral and healthy cell lines respectively. Insignificant levels of cytotoxicity were obtained by this assay when cells were cultured onto sodium hyaluronate films (Fig. 3) prepared with different amounts of crosslinker (5% and 20 wt%). It can be concluded that

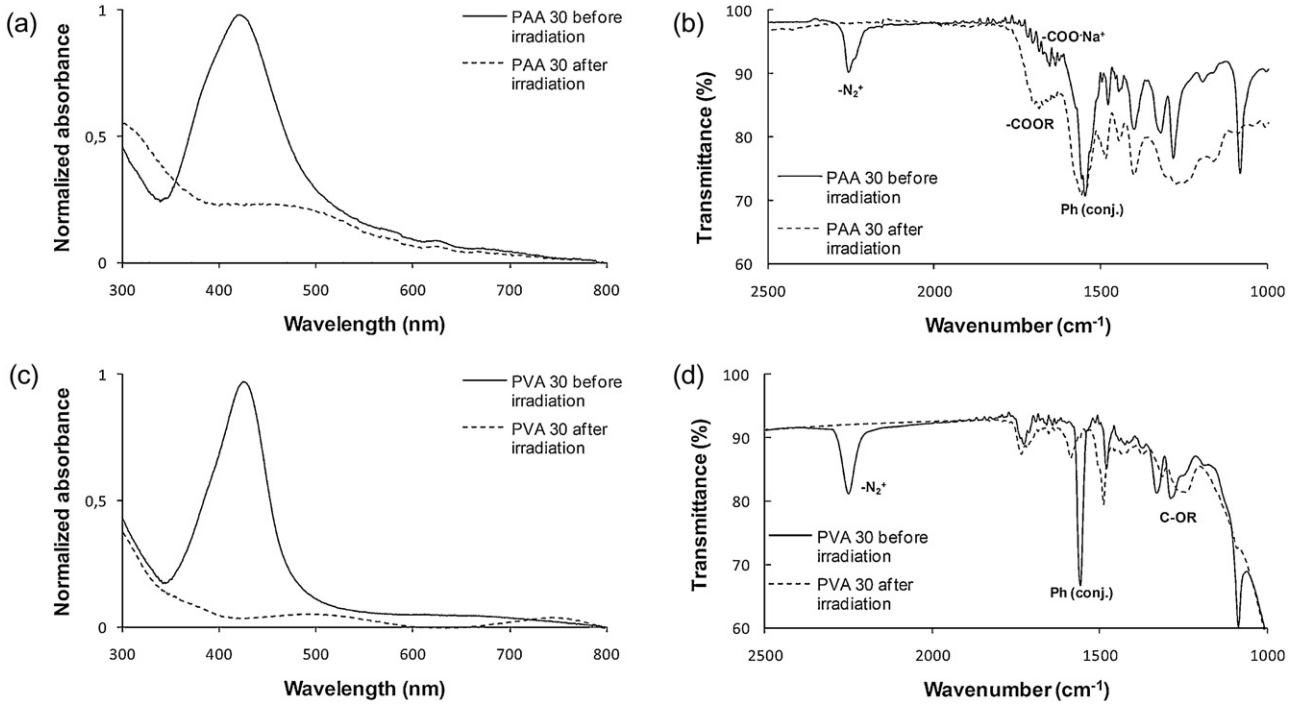


**Fig. 1.** Normalized optical absorption spectra (a and c) and FTIR spectra (b and d) of films of PAA 30 (a and b) and PVA 30 (c and d) before and after irradiation with UV light (see Section 2).

the crosslinks, resulting from the reaction of the diazonium salt, are not cytotoxic for these two cell lines.

### 3.4. 2D pattern fabrication and cell adhesion studies

Cell-substrate interactions can be modified by physico-chemical (Hervy, 2010; Scharnagl, Lee, Hiebl, Sisson, & Lendlein, 2010), biological (Hersel, Dahmen, & Kessler, 2003; Re'em, Tsur-Gang, & Cohen, 2010), and topographical (Dalby et al., 2007; Scharnagl et al., 2010; Schulte, Díez, Möller, & Lensen, 2009; Zorlutuna, Elsheikh, & Hasirci, 2009) cues and, therefore, cell adhesion and proliferation can be controlled by surface engineering. The use of light structuring techniques allows the generation of patterns with a controlled geometry and these could subsequently lead to a controlled proliferation of cells. With this aim, 2D patterns were generated by DLW on sodium hyaluronate thin films to study cell adhesion.

Patterned irradiation was performed using the DLW setup described in the experimental section. The width of the lines was set to be around typical cell dimensions in the order of 30–50 μm. In order to achieve this, the plane of the sample was placed slightly out of the focal plane. After irradiation with the laser setup, a subsequent etching step of the unexposed areas was carried out using a 0.06 M aqueous NaOH solution. The height of the resultant structures (Fig. S4 in supplementary data) was in the order of 150 nm for H5 and 400 nm for H20, lower than the film thickness before etching (500 and 1000 nm for H5 and H20 respectively). This decrease of the height after etching is ascribed to a partial removal of the polymeric material when exposed to the NaOH solution.

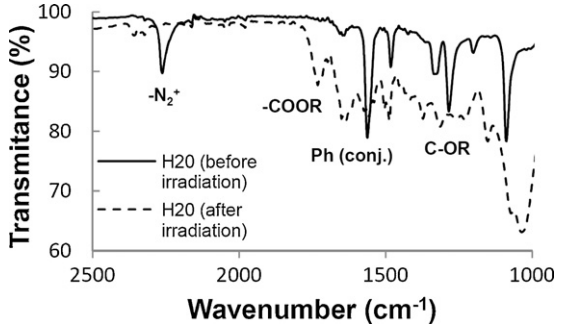


**Fig. 2.** FTIR spectra of films of H20 before and after irradiation with UV light (see Section 2).

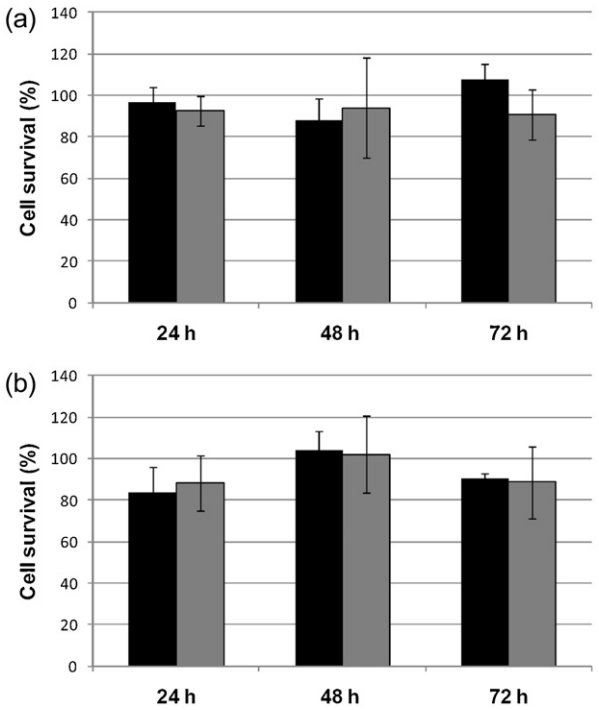


**Fig. 3.** Percentage of cell survival for HeLa tumoral cells (a) and COS-7 fibroblasts (b) cultured onto H5 (black bar) and H20 (gray bar) during 24 h, 48 h and 72 h.

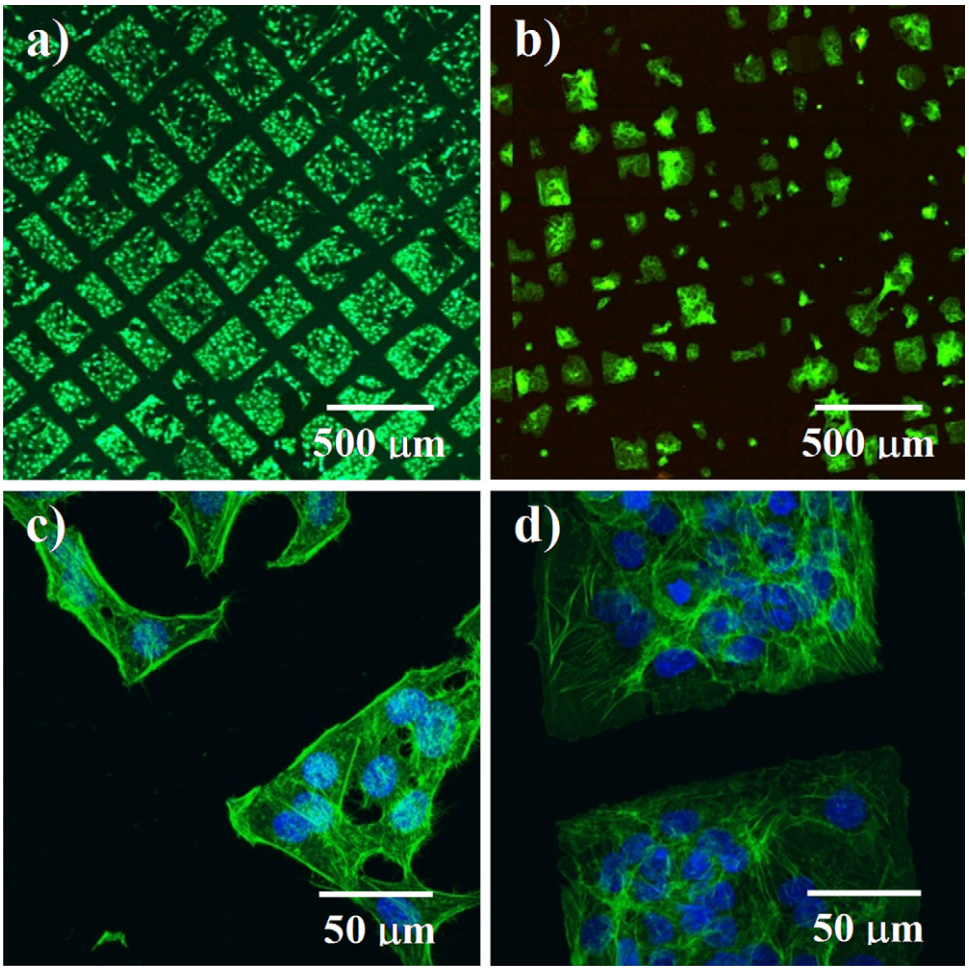


**Fig. 4.** Confocal microscopy images of fluorescent staining of actin fibers with Alexa Fluor 488 and nuclei with DAPI in HeLa tumoral cells (a and c) and COS-7 fibroblasts (b and d) onto patterned structures of H5 after 72 h of culture.

Cells were cultured on the patterned substrates to study cell adhesion onto the polymeric material. Fluorescent staining of actin fibers was performed in these cells to visualize their cytoskeleton morphology. These studies reveal that HeLa tumoral cells and COS-7 fibroblasts cultured onto microstructured H5 patterns tend to a selective adhesion to the bare glass. Fig. 4 shows square regions with the fluorescent labeled cells attached to the glass. Black stripes correspond to the polymeric lines where no cells are adhered. However, H20 patterns do not show this selective adhesion of cells to the glass and both cell lines proliferate indistinctly on the polymeric material and the glass substrate (Fig. 5). In some cases, certain orientation of the HeLa tumoral cells along the polymeric material has been observed (Fig. 5c and e).

The selective attachment of cells to bare glass regions in H5 polymeric patterned substrates was further investigated. With this aim, the culture of HeLa tumoral cells onto this kind of substrates was also monitored by sequential microscopy (see Fig. S5 in supplementary data). It was observed that cells, initially located on H5 polymeric stripes with a spherical morphology, tend to migrate to the bare glass areas in accordance with the results shown in Fig. 4.

In an attempt to gain a better understanding of the adhesion behavior in different materials, cells were cultured onto flood-exposed films of H5, H20 and glass substrates (used as a control). Focal adhesion points, which reveal cell interaction points with the surface, were labeled by fluorescent staining of vinculin fibers in cells attached onto the different substrates. Fig. 6 shows confocal microscopy images of HeLa cells (left column of Fig. 6) and COS-7 fibroblasts (right column of Fig. 6) cultured onto H5, H20 and glass substrates (1st, 2nd and 3rd row of Fig. 6, respectively). Both cell lines cultured onto H5 flood-exposed films become attached to some extent to the surface, which can explain cell viability percentages close to 100% obtained for this material. However, cells have a spherical morphology (Fig. 6a for HeLa tumoral cells and b for COS-7 fibroblasts) and show tendency to grow in colonies in the case of fibroblasts (Fig. 6b) to minimize interactions with the polymeric material H5. All these results indicate a low affinity of the cells for this material (Owen, Meredith, Gwynn, & Richards, 2005), which could be the reason of the selective cell attachment on the bare glass areas in substrates with patterned structures of H5.

When cells are cultured onto H20 flood-exposed films (Fig. 6c for HeLa tumoral cells and d for COS-7 fibroblasts), they get attached with a more extended morphology than on H5 flood-exposed films. Particularly, in the case of fibroblasts, the formation of colonies was not observed. Fig. 6d shows two COS-7 cells after division that spread over the H20 polymer surface instead of agglomerate. This extended morphology, shown by HeLa and COS-7 cells onto H20 polymeric substrates, similar to their typical morphology on glass substrate (glass is an adherent substrate for them) is due to the establishment of more focal adhesion points, which can be identified by vinculin overexpression. These results indicate a higher affinity for the most crosslinked material H20 than for the less crosslinked material H5 that behaves as a non-adherent substrate for cells (Owen et al., 2005).

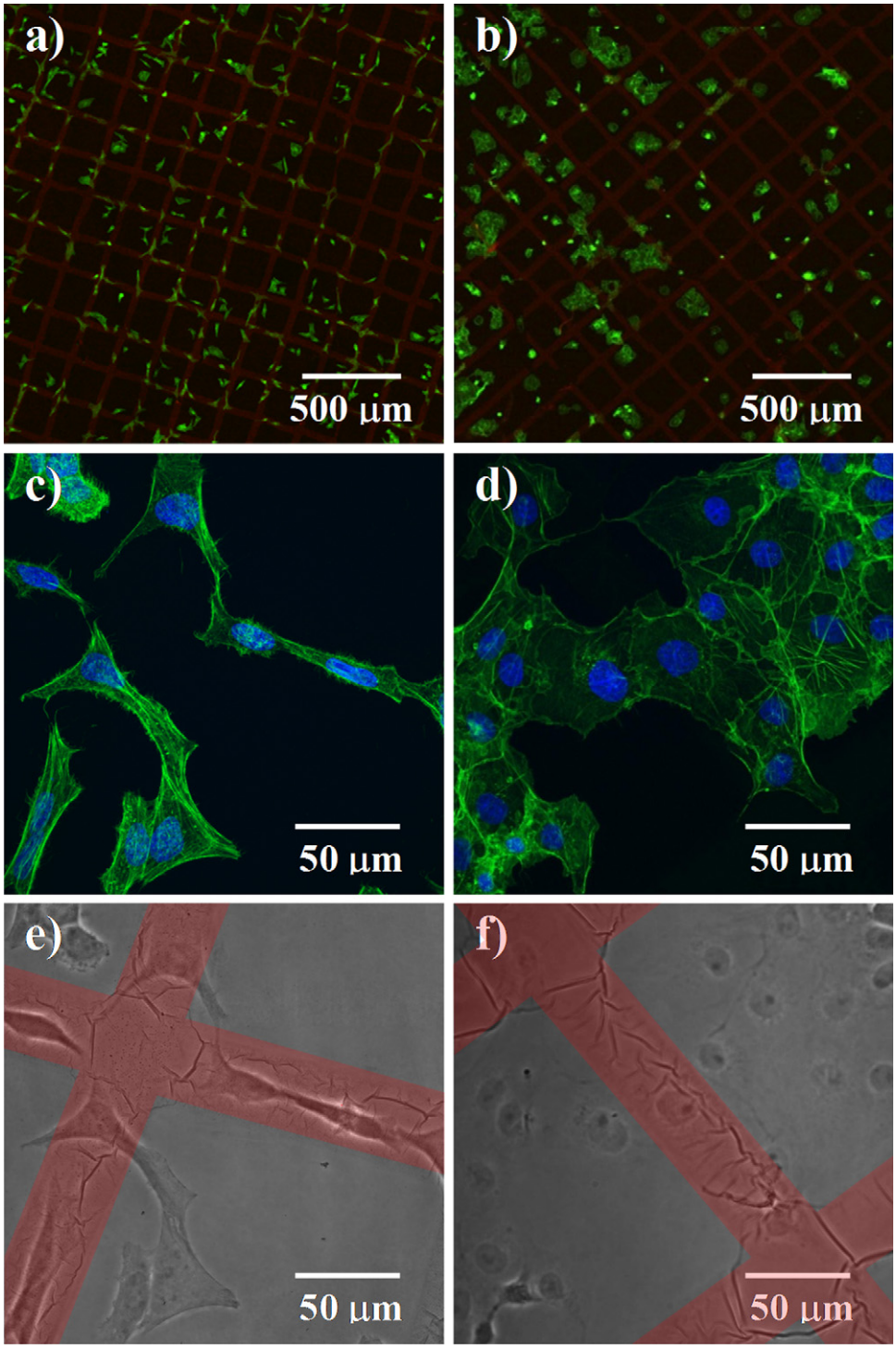


**Fig. 5.** Confocal microscopy images of fluorescent staining of actin fibers with Alexa Fluor 488 and nuclei with DAPI in HeLa tumoral cells (a, c and e) and COS-7 fibroblasts (b, d and f) onto patterned structures of H20 after 72 h of culture. Red color in (a) and (b) corresponds to the fluorescence emission from the crosslinked polymeric pattern and green staining corresponds to actin fiber staining of cells. A red stripe has been included in the 60× images (Fig. 7e and f) to indicate the location of the polymeric material. (For interpretation of the references to color in this figure legend, the reader is referred to the web version of this article.)

The spherical morphology of cells on H5 polymeric films was also characterized by scanning electron microscopy (SEM) for both cell lines (Fig. 7). When cells are cultured onto a glass substrate (as control), that is an adherent substrate, they spread their cytoplasm to establish more focal adhesion points (Fig. 7c and d, also visualized by vinculin immunostaining in Fig. 6e for HeLa tumoral cells and f for COS-7 fibroblasts). However, when they are cultured onto H5 flood-exposed polymeric films, they get attached with a spherical morphology (Fig. 7a and b) to reduce the contact and cell-surface interactions.

The different amount of crosslinker in the H5 and H20 photopolymers leads to differences in cell adhesion as demonstrated by the previously shown results. The higher content of crosslinker in H20 (with respect H5) could led to a lower extent of hydration in this material due to a higher degree of crosslinking and to a more marked reduction of the number of hydroxyl and carboxyl

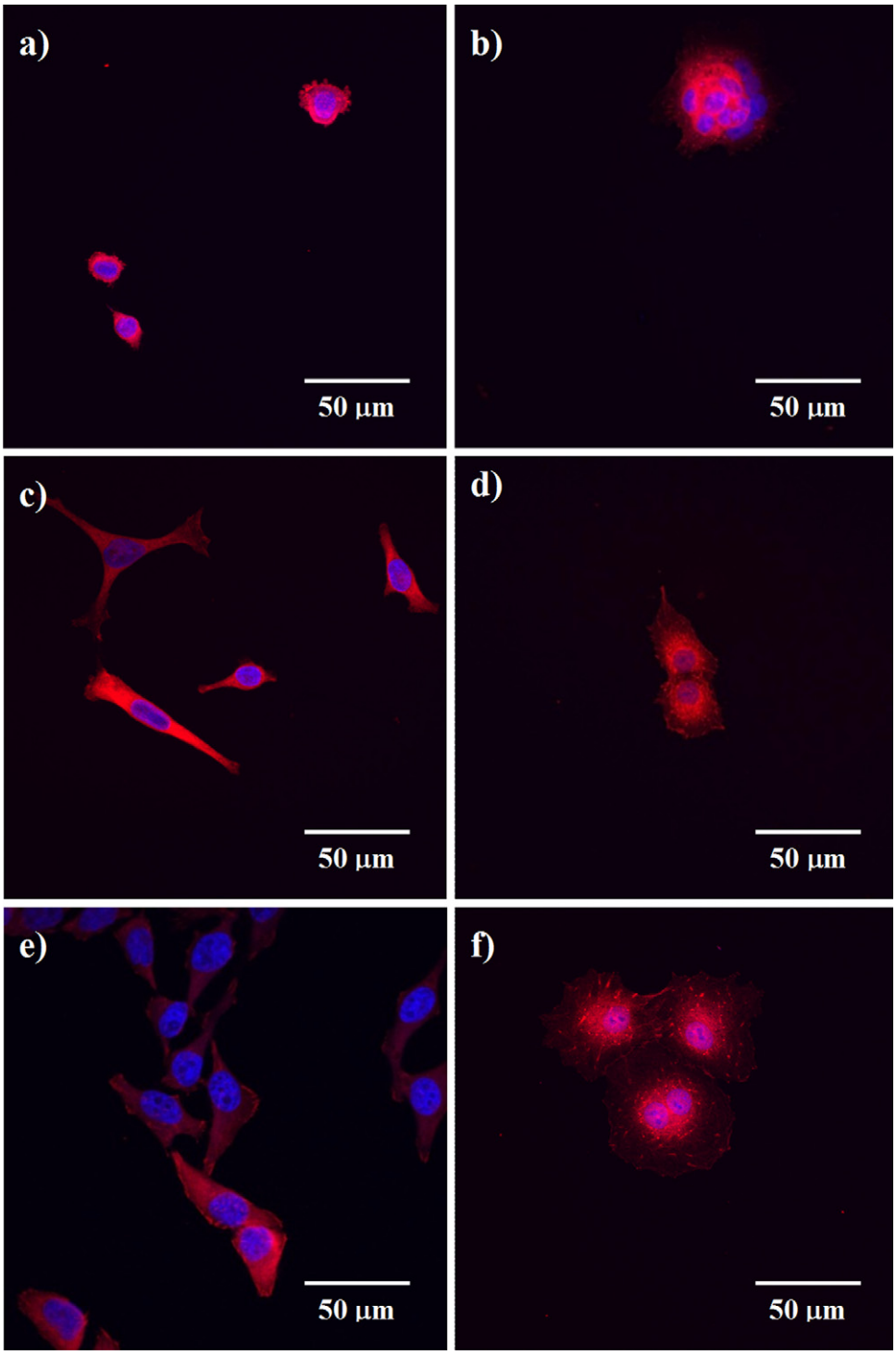


**Fig. 6.** Confocal microscopy images of fluorescent staining of vinculin fibers with Texas Red and nuclei with DAPI in HeLa tumoral cells (a, c, and e) and COS-7 fibroblasts (b, d, and f) onto flood-exposed substrates of H5 (a and b), H20 (c and d) and glass substrates (e and f) after 24 h of culture.

groups that react with the diazonium salt upon irradiation. The better adhesive properties of H20 could therefore be ascribed to a more hydrophobic character of this material when compared to H5.

The aforementioned change in cell morphology on the polymeric material H5 could be related not only with adhesion behavior but also with a cell life cycle deregulation, which may in turn lead to tumoral formation in healthy cell lines (Mahmoudi, Azadmanesh, Shokrgozar, Journeay, & Laurent, 2011). Additionally, spherical morphology is typical in apoptotic dying cells (Willingham, 1999). In order to discard cycle deregulation or apoptosis, the cell life cycle was analyzed by flow cytometry for cells cultured onto H5 polymeric films and cells cultured onto glass substrates as control of normal cell population.

Typically, two peaks are observed in graphs obtained in this cell life cycle analysis. The main peak corresponds to cells in the $G_0$–$G_1$ phase (non-dividing cells) and the second peak, assigned to cells in the $G_2$-M phase (dividing cells), appears at double the fluorescence intensity ($X$ axis) because of the double DNA content (Mahmoudi et al., 2011). Between these two peaks, there is a

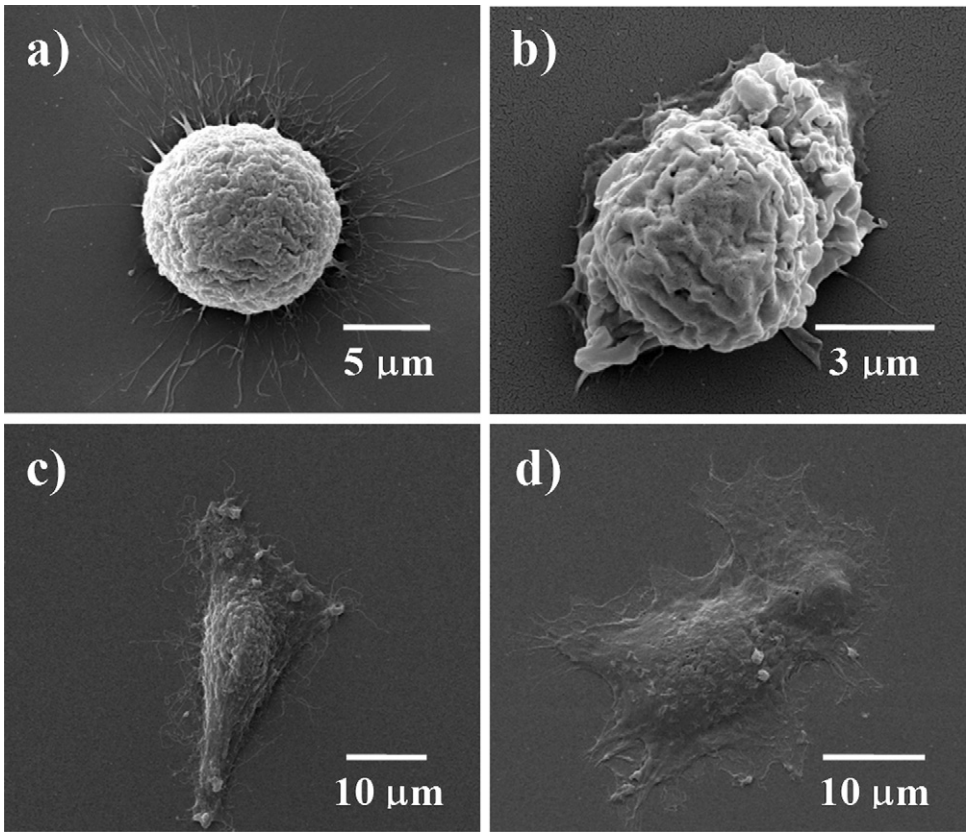


**Fig. 7.** Scanning electron microscopy (SEM) images of HeLa tumoral cells (a and c) and COS-7 fibroblasts (b and d) cultured onto flood-exposed substrates of H5 (a and b) and glass substrates (c and d).

plateau that is assigned to cells that are replicating DNA during the synthesis phase (S) and they have different amounts of DNA. Apoptotic cells can also be identified because they lose nucleic material and another peak can be observed at lower fluorescence intensity than the $G_0$–$G_1$ peak (sub $G_0$–$G_1$ peak) (Mahmoudi et al., 2009).

As we can see in Table 1, percentage of HeLa tumoral cells in the S phase is lower when they are cultured on H5 polymeric films than those cultured on glass substrates. In turn, a higher percentage of HeLa tumoral cells in the $G_0$–$G_1$ phase is found in H5 polymeric films in comparison to glass substrates. These data reveals that hyaluronate-based polymeric material H5 slows down the DNA synthesis process in HeLa tumoral cells. The percentage of HeLa tumoral cells in $G_2$-M phase is similar when they are cultured on H5 polymeric films or glass substrates, what is consistent with the similar cell survival percentages obtained by MTT cell proliferation assay. For COS-7 fibroblasts, studied as model of healthy line, the percentage of cells in all the life cycle phases are similar when they are cultured on H5 polymeric films and glass substrates. These results indicate that H5 do not deregulate COS-7 fibroblasts normal life cycle in spite of the change of morphology experimented by COS-7 fibroblasts cultured on this material. The similar percentage of cells in $G_2$-M is also consistent with the cell survival percentages (close to 100%) obtained by MTT cell proliferation assay for COS-7 fibroblasts. Additionally, no sub $G_0$–$G_1$ peak was found for any of the studied cell lines, which indicates the absence of apoptotic cells and, therefore, that the studied material H5 is not cytotoxic for none of them.

**Table 1**
Percentage of cell cycle phases for HeLa tumoral cells and COS-7 fibroblasts cultured onto H5 polymeric films or glass substrates respectively (cell culture time: 24 h).

| Sample | $G_0$–$G_1$ [%] | S [%] | $G_2$-M [%] | $G_2$-M/$G_0$–$G_1$ [%] |
|---|---|---|---|---|
| HeLa H5 | 75.03 | 19.14 | 5.83 | 0.08 |
| HeLa control | 57.77 | 35.61 | 6.61 | 0.11 |
| COS-7 H5 | 47.31 | 37.77 | 14.92 | 0.32 |
| COS-7 control | 48.10 | 39.29 | 12.61 | 0.26 |

## 4. Conclusions

The photoinduced reaction of diazonium salts has been applied to generate polymeric biomaterials through light-induced crosslinking of chemically unmodified sodium hyaluronate with a trifunctional low molecular weight diazonium salt as crosslinker. The reaction was investigated with the model polymers PAANa and PVA, which contain similar nucleophilic groups as sodium hyaluronate. The photoinduced process was characterized by UV–vis absorption and FTIR spectroscopy, and the reaction between crosslinker and polymers was confirmed for all polymeric materials, including sodium hyaluronate.

Cell proliferation on flood-exposed substrates of crosslinked sodium hyaluronate films, obtained using the diazonium salt as photocrosslinker, was studied by MTT cell proliferation assays with two different cell lines (HeLa tumoral cells and COS-7 fibroblasts). Sodium hyaluronate-based materials H5 and H20, which have different crosslinker percentages, did not show cytotoxicity.

Photocrosslinkable thin films were deposited on glass substrates and patterned by direct laser writing to obtain stable 2D polymeric patterns for H5 and H20. Cell adhesion studies onto these polymeric patterns showed a selective attachment of both cell lines (HeLa tumoral cells and COS-7 fibroblasts) on the bare glass areas in the case of H5 polymeric patterns, what is assigned to a low affinity for the lowest crosslinked material H5. This low affinity leads cells (HeLa tumoral cells and COS-7 fibroblasts) to acquire a spherical morphology when they are cultured onto flood-exposed films of H5

in order to minimize interactions with the surface of the polymeric material. The lower content of crosslinker in this H5 material could lead to a more hydrated and therefore non-adherent system leading to this change in cell morphology. This change was accompanied by a slight deregulation of cell life cycle only for HeLa tumoral, where synthesis of DNA was slowed down. For COS-7 fibroblasts, no alteration of cell life cycle was observed, what indicates that H5 has an effect only in the cell adhesion behavior but not in the cell life cycle. Therefore the adhesive/antiadhesive balance could be tuned (without affecting the cell life cycle in the case of COS-7 fibroblasts) by controlling the amount of crosslinker.

In summary, the direct photocrosslinking of sodium hyaluronate with multifunctional diazonium salt crosslinkers has been demonstrated to be a feasible approach for the preparation of biomaterials without the need for a photoinitiator or the chemical functionalization of the natural polymer. This reaction could also be used to generate biomaterials from other natural polymers that contain nucleophilic groups such as sodium heparin. For sodium hyaluronate films, cell adhesion can be tune by modifying the crosslinker percentage of photocrosslinkable formulation. This allows to modify cell adhesion behavior that can be locally controlled by applying light structuring techniques.

## Acknowledgements

This work was supported by the Spanish MEC project MAT2011-27978-C02 and MAT2011-26851-C02-01, ARAID project for young scientists, ERC-Starting Grant NANOPUZZLE and FEDER funding (EU). M. Lomba thanks the Gobierno de Aragón (Spain) for a PhD. Grant. JM de la Fuente thanks ARAID for financial support. B. Saez Gutiérrez thanks ISCIII for financial support (Sara Borrell CD09/00174).

The authors thank Dr. M. Royo (Microscopy and Image Service) and Dr. J. Godino (Cellular Separation and Cytometry) for technical assistance and help with the confocal microscope and flow cytometry analyses, respectively, and the I+CS/IIS Aragon (Aragon Health Sciences Institute) for access to the microscope and the flow cytometer. The authors also thank the Institute of Nanoscience of Aragon (INA) for access to the scanning electron microscope, and Carlos Cuesta from Advanced Microscopy Laboratory for the technical support. Finally, the authors thank Dr. L. Álvarez-Vallina of the Hospital Puerta de Hierro (Madrid) for HeLa tumoral cells.

## Appendix A. Supplementary data

Supplementary data associated with this article can be found, in the online version, at http://dx.doi.org/10.1016/j.carbpol.2012.05.061.

## References

Badylak, S. F., Freytes, D. O., & Gilbert, T. W. (2009). Extracellular matrix as a biological scaffold material: Structure and function. *Acta Biomater*, *5*, 1–13.

Baroli, B. (2006). Photopolymerization of biomaterials: Issues and potentialities in drug delivery, tissue engineering, and cell encapsulation applications. *Journal of Chemical Technology and Biotechnology*, *81*, 491–499.

Bencherif, S. A., Srinivasan, A., Horkay, F., Hollinger, J. O., Matyjaszewski, K., & Washburn, N. R. (2008). Influence of the degree of methacrylation on hyaluronic acid hydrogels properties. *Biomaterials*, *29*, 1739–1749.

Bratton, D., Yang, D., Dai, J., & Ober, C. K. (2006). Recent progress in high resolution lithography. *Polymers for Advanced Technologies*, *17*, 94–103.

Burdick, J. A., & Prestwich, G. D. (2011). Hyaluronic acid hydrogels for biomedical applications. *Advanced Materials*, *23*, H41–H56.

Camci-Unal, G., Aubin, H., Ahari, A. F., Bae, H., Nichol, J. W., & Khademhosseini, A. (2010). Surface-modified hyaluronic acid hydrogels to capture endothelial progenitor cells. *Soft Matter*, *6*, 5120–5126.

Cao, S., Zhao, C., & Cao, W. (1998). Synthesis of diazoresin and its photocrosslinking reaction. *Polymer International*, *45*, 142–146.

Cao, T., Yang, S., Cao, J., Zhang, M., Huang, C., & Cao, W. (2001). Nanoassembly film of carboxylic polyaniline with photosensitive diazoresin and its photoelectric conversion properties. *Journal of Physical Chemistry B*, *105*, 11941–11944.

Cao, T., Yang, S., Yang, Y., Huang, C., & Cao, W. (2001). Photoelectric conversion property of covalent-attached multilayer self-assembled films fabricated from diazoresin and fullerol. *Langmuir*, *17*, 6034–6036.

Cao, W. X., Ye, S. J., Cao, S. G., & Zhao, C. (1997). Novel polyelectrolyte complexes based on diazo-resins. *Macromolecular Rapid Communications*, *18*, 983–989.

Censi, R., Fieten, P. J., di Martino, P., Hennink, W. E., & Vermonden, T. (2010). In situ forming hydrogels by tandem thermal gelling and Michael addition reaction between thermosensitive triblock copolymers and thiolated hyaluronan. *Macromolecules*, *43*, 5771–5778.

Chen, W. Y. J., & Abatangelo, G. (1999). Functions of hyaluronan in wound repair. *Wound Repair and Regeneration*, *7*, 79–89.

Chen, J., & Cao, W. (1999). Fabrication of a covalently attached self-assembly multilayer film via H-bonding attraction and subsequent UV-irradiation. *Chemical Communications*, 1711–1712.

Dalby, M. J., Gadegaard, N., Tare, R., Andar, A., Riehle, M. O., Herzyk, P., Wilkinson, C. D. W., & Oreffo, R. O. C. (2007). The control of human mesenchymal cell differentiation using nanoscale symmetry and disorder. *Nature Materials*, *6*, 997–1003.

Dutta, R. C., & Dutta, A. K. (2010). Comprehension of ECM-Cell dynamics: A prerequisite for tissue regeneration. *Biotechnology Advances*, *28*, 764–769.

Fridovich, I. (1998). Oxygen toxicity: A radical explanation. *Journal of Experimental Biology*, *201*, 1203–1209.

Friedl, P., Zänker, K. S., & Bröcker, E. B. (1998). Cell migration strategies in 3-D extracellular matrix: Differences in morphology, cell matrix interactions, and integrin function. *Microscopy Research and Technique*, *43*, 369–378.

Gomes, M. E., & Reis, R. L. (2004). Biodegradable polymers and composites in biomedical applications: From catgut to tissue engineering, Part 1: Available systems and their properties. *International Materials Reviews*, *49*, 261–273.

Hersel, U., Dahmen, C., & Kessler, H. (2003). RGD modified polymers: Biomaterials for stimulated cell adhesion and beyond. *Biomaterials*, *24*, 4385–4415.

Hervy, M. (2010). Modulation of cell structure and function in response to substrate stiffness and external forces. *Journal of Adhesion Science and Technology*, *24*, 963–973.

Hoare, T. R., & Kohane, D. S. (2008). Hydrogels in drug delivery: Progress and challenges. *Polymer*, *49*, 1993–2007.

Hoyle, C. E., & Bowman, C. N. (2010). Thiol-ene click chemistry. *Angewandte Chemie International Edition*, *49*, 1540–1573.

Inukai, M., Jin, Y., Yomota, C., & Yonese, M. (2000). Preparation and characterization of hyaluronate-hydroxyethyl acrylate blend hydrogel for controlled release device. *Chemical and Pharmaceutical Bulletin*, *48*, 850–854.

Ji, Y., Ghosh, K., Li, B., Sokolov, J. C., Clark, R. A. F., & Rafailovich, M. H. (2006). Dual-syringe reactive electrospinning of cross-linked hyaluronic acid hydrogel nanofibers for tissue engineering applications. *Macromolecular Bioscience*, *6*, 811–817.

Khetan, S., & Burdick, J. A. (2011). Patterning hydrogels in three dimensions towards controlling cellular interactions. *Soft Matter*, *7*, 830–838.

Kim, J., Park, Y., Tae, G., Lee, K. B., Hwang, C. M., Hwang, S. J., Kim, I. S., Noh, I., & Sun, K. (2009). Characterization of low-molecular-weight hyaluronic acid-based hydrogel and differential stem cell responses in the hydrogel microenvironments. *Journal of Biomedical Materials Research A*, *88*, 967–975.

Kutty, J. K., Cho, E., Lee, J. S., & Vyavahare, N. R. (2007). Webb K. the effect of hyaluronic acid incorporation on fibroblast spreading and proliferation within PEG-diacrylate based semi-interpenetration networks. *Biomaterials*, *28*, 4928–4938.

Lei, Y., Gojgini, S., Lam, J., & Segura, T. (2011). The spreading, migration and proliferation of mouse mesenchymal stem cells cultured inside hyaluronic acid hydrogels. *Biomaterials*, *32*, 39–47.

Li, Q., Ouyang, J., Chen, J., Zhao, X., & Cao, W. (2002). Photosensitive, self-assembled ultrathin films based on diazoresin and phosphate-containing polyanions. *Journal of Polymer Science Part A: Polymer Chemistry*, *40*, 222–228.

Liu, J. H., Lee, S. Y., & Tsai, F. R. (1998). Synthesis and characterization of photocrosslinkable poly(amic acid-co-urea)s with diazoresin. *Journal of Applied Polymer Science*, *770*, 2401–2407.

Lomba, M., Oriol, L., Alcalá, R., Sánchez, C., Moros, M., Grazú, V., Serrano, J. L., & De la Fuente, J. M. (2011). In situ photopolymerization of biomaterials by thiol-yne click chemistry. *Macromolecular Bioscience*, *11*, 1505–1514.

Lomba, M., Oriol, L., & Sánchez, C. (2009). A new photoimaging system based on a trisdiazonium salt as a photocrosslinker for sulfonated polyelectrolytes. *European Polymer Journal*, *45*, 1785–1790.

Lowe, A. B., Hoyle, C. E., & Bowman, C. N. (2010). Thiol-yne click chemistry: A powerful and versatile methodology for materials synthesis. *Journal of Materials Chemistry*, *20*, 4745–4750.

Mahmoudi, M., Azadmanesh, K., Shokrgozar, M. A., Journeay, W. S., & Laurent, S. (2011). Effect of nanoparticles on the cell life cycle. *Chemical Reviews*, *111*, 3407–3432.

Mahmoudi, M., Simchi, A., Vali, H., Imani, M., Shokrgozar, M. A., Azadmanesh, K., & Azari, F. (2009). Cytotoxicity and cell cycle effects of bare and poly(vinylalcohol)-coated iron oxide nanoparticles in mouse fibroblasts. *Advanced Engineering Materials*, *11*, B243.

Malafaya, P. B., Silva, G. A., & Reis, R. L. (2007). Natural-origin polymers as carriers and scaffolds for biomolecules and cell delivery in tissue engineering applications. *Advanced Drug Delivery Reviews*, *59*, 207–233.

Masters, K. S., Shah, D. N., Leinwand, L. A., & Anseth, K. S. (2005). Crosslinked hyaluronan scaffolds as a biologically active carrier for valvular interstitial cells. *Biomaterials*, *26*, 2517–2525.

Mosmann, T. (1983). Rapid colorimetric assay for cellular growth and survival: Application to proliferation and cytotoxicity assays. *Journal of Immunological Methods*, *65*, 55–63.

Nuernberger, S., Cyran, N., Albrecht, C., Redl, H., Vécsei, V., & Marlovits, S. (2011). The influence of scaffold architecture on chondrocyte distribution and behavior in matrix-associated chondrocyte transplantation grafts. *Biomaterials*, *32*, 1032–1040.

Oh, J. K., Drumright, R., Siegwart, D. J., & Matyjaszewski, K. (2008). The development of microgels/nanogels for drug delivery applications. *Progress in Polymer Science*, *33*, 448–477.

Owen, G. R., Meredith, D. O., Gwynn, I., & Richards, R. G. (2005). Focal adhesion quantification – A new assay of material biocompatibility: Review. *European Cells & Materials*, *9*, 85–96.

Patterson, J., Siew, R., Herring, S. W., Lin, A. S. P., Guldberg, R., & Stayton, P. S. (2010). Hyaluronic acid hydrogels with controlled degradation properties for oriented bone regeneration. *Biomaterials*, *31*, 6772–6781.

Perng, C. K., Wang, Y. J., Tsi, C. H., & Ma, H. (2011). In vivo angiogenesis effect of porous collagen scaffold with hyaluronic acid oligosaccharides. *Journal of Surgical Research*, *168*, 9–15.

Raines, A. L., Sunwoo, M. H., Gertzman, A. A., Thacker, K., Guldberg, R. E., Schwartz, Z., & Boyan, B. D. (2011). Hyaluronic acid stimulates neovascularization during the regeneration of bone marrow after ablation. *Journal of Biomedical Materials Research A*, *96*, 575–583.

Re'em, T., Tsur-Gang, O., & Cohen, S. (2010). The effect of immobilized RGD peptide in macroporous alginate scaffolds on TGFβ1-induced chondrogenesis of human mesenchymal stem cells. *Biomaterials*, *31*, 6746–6755.

Rhydolm, A. E., Bowman, C. N., & Anseth, K. S. (2005). Degradable thiol-acrylate photopolymers: Polymerization and degradation behavior of an in situ forming biomaterial. *Biomaterials*, *26*, 4495–4506.

Rhydolm, A. E., Reddy, S. K., Anseth, K. S., & Bowman, C. N. (2007). Development and characterization of degradable thiol-allyl ether photopolymers. *Polymer*, *48*, 4589–4600.

Rinaudo, M. (2008). Main properties and current applications of some polysaccharides as biomaterials. *Polymer International*, *57*, 397–430.

Scharnagl, J., Lee, S., Hiebl, B., Sisson, A., & Lendlein, A. (2010). Design principles for polymers as substratum for adherent cells. *Journal of Materials Chemistry*, *20*, 8789–8802.

Schulte, V. A., Díez, M., Möller, M., & Lensen, M. C. (2009). Surface topography induces fibroblast adhesion on intrinsically nonadhesive poly(ethylene glicol) substrates. *Biomacromolecules*, *10*, 2795–2801.

Seidlits, S. K., Schmidt, C. E., & Shear, J. B. (2009). High-resolution patterning of hydrogels in three dimensions using direct-write photofabrication for cell guidance. *Advanced Functional Materials*, *19*, 3543–3551.

Senyurt, A. F., Wei, H., Hoyle, C. E., Piland, S. G., & Gould, T. E. (2007). Ternary thiol-ene/acrylate photopolymers: Effect of acrylate structure on mechanical properties. *Macromolecules*, *40*, 4901–4909.

Srivastava, R., Brown, J. Q., Zhu, H., & McShane, M. J. (2005). Stabilization of glucose oxidase in alginate microspheres with photoreactive diazoresin nanofilm coatings. *Biotechnology and Bioengineering*, *91*, 124–131.

Sun, J., Wu, T., Sun, Y., Wang, Z., Zhang, X., Shen, J., & Cao, W. (1998). Fabrication of a covalently attached multilayer via photolysis of layer-by-layer self-assembled films containing diazo-resins. *Chemical Communications*, 1853–1854.

Tomihata, K., & Ikada, Y. (1997). Crosslinking of hyaluronic acid with water-soluble carbodiimide. *Journal of Biomedical Materials Research A*, *37*, 243–251.

Van Tomme, S. R., Storm, G., & Hennink, W. E. (2008). In situ gelling hydrogels for pharmaceutical and biomedical applications. *International Journal of Pharmaceutics*, *355*, 1–18.

Vercruysse, K. P., Marecak, D. M., Marecek, J. F., & Prestwich, G. D. (1997). Synthesis and in vitro degradation of new polyvalent hydrazide cross-linked hydrogels of hyaluronic acid. *Bioconjugate Chemistry*, *8*, 686–694.

Willingham, M. C. (1999). Cytochemical methods for the detection of apoptosis. *Journal of Histochemistry and Cytochemistry*, *47*, 1101–1109.

Yu, B., Cong, H. L., Liu, H. W., Lu, C. H., Wei, F., & Cao, W. X. (2006). Fabrication and characterization of stable ultrathin film micropatterns containing DNA and photosensitive polymer diazoresin. *Analytical and Bioanalytical Chemistry*, *384*, 385–390.

Zhang, Y., & Cao, W. (2000). A novel photosensitive ternary complex consisting of phenol-formaldehyde resin, sodium dodecyl sulfate, and diazo resin. *Journal of Polymer Science Part A: Polymer Chemistry*, *38*, 2566–2571.

Zhang, L., Peng, Z., Yao, L., Ly, F., & Xuan, L. (2007). Photoalignment of liquid crystals using a covalently attached self-assembled ultrathin film fabricated from diazoresin and cinnamate polyelectrolyte. *Journal of Materials Chemistry*, *17*, 3015–3022.

Zhao, S., Zhang, K., Yang, M., Sun, Y., & Sun, C. (2006). Fabrication of photosensitive self-assembled multilayer films based on porphyrin and diazoresin via H-bonding. *Materials Letters*, *60*, 2406–2409.

Zorlutuna, P., Elsheikh, A., & Hasirci, V. (2009). Nanopatterning of collagen scaffolds improve the mechanical properties of tissue engineered vascular grafts. *Biomacromolecules*, *10*, 814–821.